



DEPARTMENT of ARTIFICIAL INTELLIGENCE

The University of Edinburgh  
5 Forrest Hill  
Edinburgh EH1 2QL

Fax 031 225 9370

Telex 727442 (UNIVED G)

Email

Telephone 031 650 1000

or direct dial 031 650

Dear Professor Howe,

As author/co-author (and copyright holder of) Research Paper No.

"Rejection of Spurious Reflections in Structured Illumination  
Range Finders"

reproduced by the Department of Artificial Intelligence,  
University of Edinburgh, relating to work carried out  
during my period of employment/study at the University of  
Edinburgh, I grant the University the right to reproduce  
and distribute copies of this paper, including the right  
to make charges therefor. I also grant the University the  
right to make agreements with third parties to reproduce  
this paper and distribute copies, including the right to make  
charges therefor.

Finally I agree to waive my right to any financial reimbursement  
from any proceeds of any sales of this paper.

Yours sincerely,

(Robert B Fisher)

(D. Kaliprasad Naidu)

(Deepak Singhal)



DEPARTMENT of ARTIFICIAL INTELLIGENCE

The University of Edinburgh

5 Forrest Hill

Edinburgh EH1 2QL

Fax 031 225 9370

Telex 727442 (UNIVED G)

Email

Telephone 031 650 1000

or direct dial 031 650

Dear Deepak:

Enclosed is a copy of the paper that  
is being presented at

2nd Conf on Optical 3-D

Measurement Techniques, Zurich, Oct 4-7

I hope you're well.

Bob Fisher

# Rejection Of Spurious Reflections In Structured Illumination Range Finders

Robert B. Fisher, D. Kaliprasad Naidu and Deepak Singhal

Department of Artificial Intelligence

University of Edinburgh

5 Forrest Hill

Edinburgh, Scotland, UK

### Abstract

This paper describes techniques for two (or more) camera geometry structured illumination range finders that eliminates most spurious range values that arise from specular reflections from shiny (e.g. metallic) parts. The key observation is that specular reflections produce range values that depend on camera position. Hence, by using two cameras, several consistency tests can be applied that eliminate most spurious range data. This paper describes the constraints that underly the tests and shows sample performance.

## 1 Introduction

The last ten years have seen many different triangulation based range sensors based on structured illumination. (A good survey is in [1]. Some other specific sensors are: [3], [4], [5].) The illumination process (e.g. a projected plane of light) makes it possible to readily locate a set of scene points that satisfy some geometric constraint (e.g. all lie in a known plane) and the observation of the illuminated points generates another geometric constraint (e.g. the three dimensional lines-of-sight to the observed points). Combination of the constraints defines the three-dimensional position of the illuminated point through simple geometric triangulation calculations. However, all techniques depend on correctly locating the illuminated features, which is problematic on surfaces that easily reflect light.

Many potential applications of these range-finders are in industrial or autonomous vehicle settings where the objects that are to be scanned are made of metal or plastic. This means that there is likely to be light specularly reflecting from "shiny" surfaces. If the parts are highly polished, then usually no light stripe will be observed from the true surfaces and the method is not usable. However, in more typical applications, where the surface is merely machined, stamped or moulded, it is possible to observe the stripe

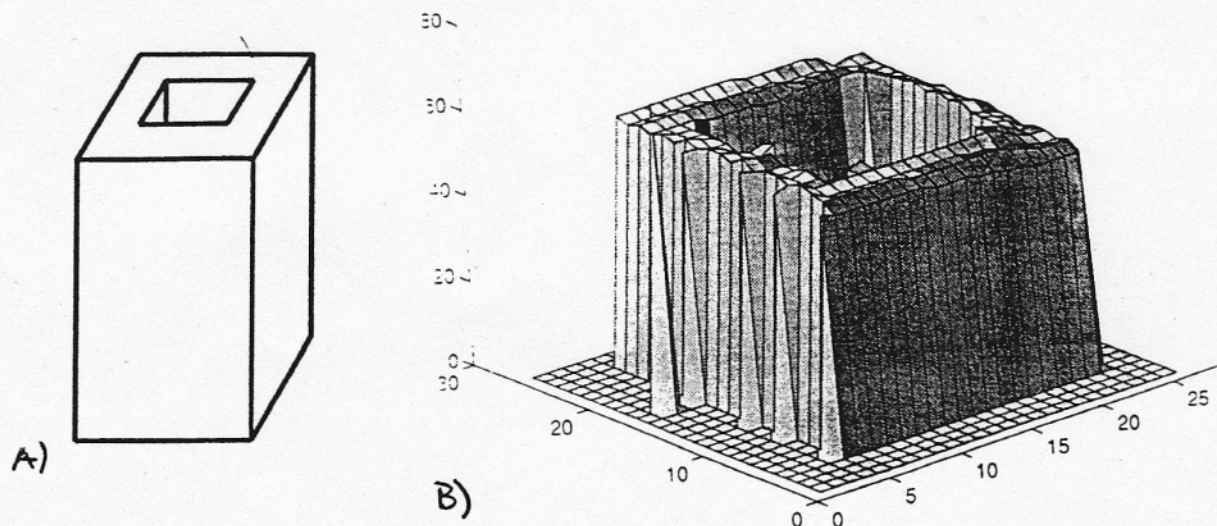


Figure 1: A simple object and its true range surface

on the surface. Unfortunately, when surfaces have a specular component, there are also many reflections of the illumination. When these reflections are observed and are treated as if they were the primary reflection, then false range values will result. For example, Figure 1 part (a) shows a simple surface with a hole. A good range image for this part is shown in Figure 1 part (b). However, when applying the usual single camera range finding method, the range image obtained is Figure 2 part (a). Note that there is a false surface observed in the center of the hole. This arises from observing reflections from the side of the hole, rather than the true stripe on the bottom of the hole.

This paper shows that there are simple techniques based on two (or more) camera geometries that can eliminate most of the spurious range values. The key observation is that specular reflections produce range values that depend on camera position. Hence, using two cameras allows the comparison of the range values from the two cameras and elimination of points where the range values are inconsistent.

The mechanical layout of the cameras nor the use of two cameras is not original; however, the method of using the discrepancy between the observed range values to eliminate data arising from spurious reflections is.

## 2 Principles of Operation

Most active illumination range sensors are based on a single camera geometry. If two cameras were used, then two range values would be observed for each illuminated point on the object being sensed, assuming that the illumination were observable by both cameras. This section describes a two camera sensor that uses a fixed light plane as the illumination. The part being scanned passes sequentially underneath the sensor to produce a full range image. When both cameras observe the stripe, then several consistency tests are applied to the data. Note that the tests are also applicable if the object is fixed and the light plane is swept.

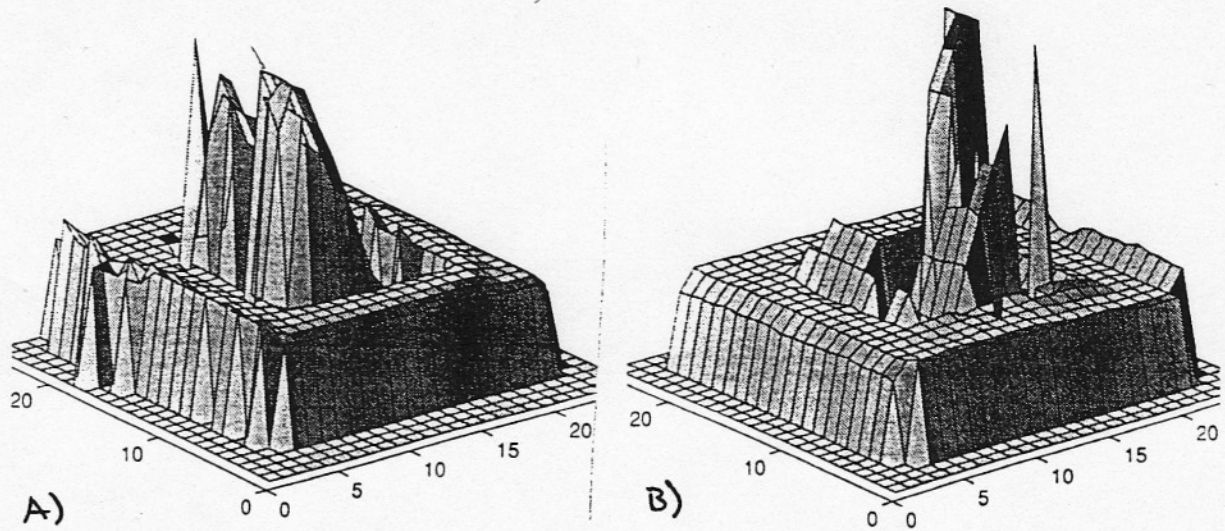


Figure 2: A false range surface for the same specular surface when observed from the (a) left and (b) right cameras

## 2.1 Sensor Geometry

The main principles of a triangulation range sensor operation are:

1. The light plane is the set of points  $\{\vec{X}_i\}$  defined:

$$\vec{X} \circ \vec{N}_{LP} = d_{LP}$$

where  $\vec{N}_{LP}$  is the unit normal to the stripe plane and  $d_{LP}$  is an appropriate scalar.

2. The object to be measured intersects the light plane such that a stripe of light is produced on the object. The light stripe is observed by two opposing cameras at positions  $\vec{O}_L$  and  $\vec{O}_R$  (left (L) and right (R) cameras respectively) producing two images containing the stripe. Note, for the best application of the rejection techniques described in this paper, the cameras must be on opposite sides of the illumination.
3. There is an image position of each stripe point  $\vec{I}_L(t)$  and  $\vec{I}_R(t)$  from the left and right images, where  $t$  indexes along the stripe.
4. For each  $t$ , the point  $\vec{I}_\alpha(t)$  determines (where  $\alpha$  is either  $L$  or  $R$ ) a ray in space that passes through the camera origin  $\vec{O}_\alpha$  and the three-dimensional spatial point  $\vec{P}_\alpha(t)$  on the camera's image plane that corresponds to the observed two-dimensional stripe point  $\vec{I}_\alpha(t)$ . This ray is:

$$\vec{R}_\alpha(t, \lambda) = \vec{O}_\alpha + \lambda(\vec{P}_\alpha(t) - \vec{O}_\alpha)$$

5. The three dimensional position of each point  $(X_\alpha(t), Y_\alpha(t), Z_\alpha(t))$  on the object is calculated by solving for the intersection of the ray and the light plane, i.e. by finding  $\lambda$  such that:

$$\vec{R}_\alpha(t, \lambda) \circ \vec{N}_{LP} = d_{LP}$$

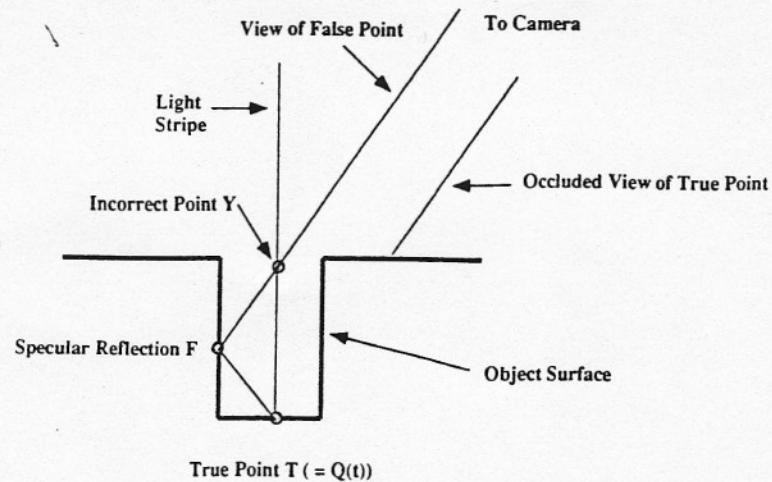


Figure 3: How specular reflections cause false range values

## 2.2 Source of Spurious Range Values

We will now see how reflections from specular surfaces can cause spurious range values. Suppose that the light stripe reflects from a specular surface and is observed, as shown in Figure 3. This shows a cross section perpendicular to the light plane, through a rectangular hole in the object surface. Here, the specular reflection at point **F** is observed rather than the true point **T**. The false point might be chosen because it might be brighter (often possible on specular surfaces) or the true point may be hidden.

The triangulation calculation will infer that the observed stripe point must lie at **Y** instead of **T**. The false range surface shown in Figure 2 part (a) resulted from this phenomena occurring at many positions along each of many stripes. The tilting false surface arises because, as the stripe moves away from the wall, the triangulated false position moves further away from the true surface. This simple false surface pattern arises from the simple rectangular hole geometry. More complex holes or combinations of specular surfaces produce more complex artifacts.

Figure 2 part (b) shows the same false results when observed from the right camera. The fact that there is a difference between the two false images lays the foundation for the spurious range value suppression techniques presented in the next subsection.

## 3 Elimination of False Range Values

The rejection of false range values is based on the constraints described below. Any points that do not satisfy the constraints are eliminated.

- **Illumination Direction Constraint**

Assuming that the stripe plane illumination projects from fixed directions (either orthographically or perspectively), it is not possible for a "beam" of light to intersect

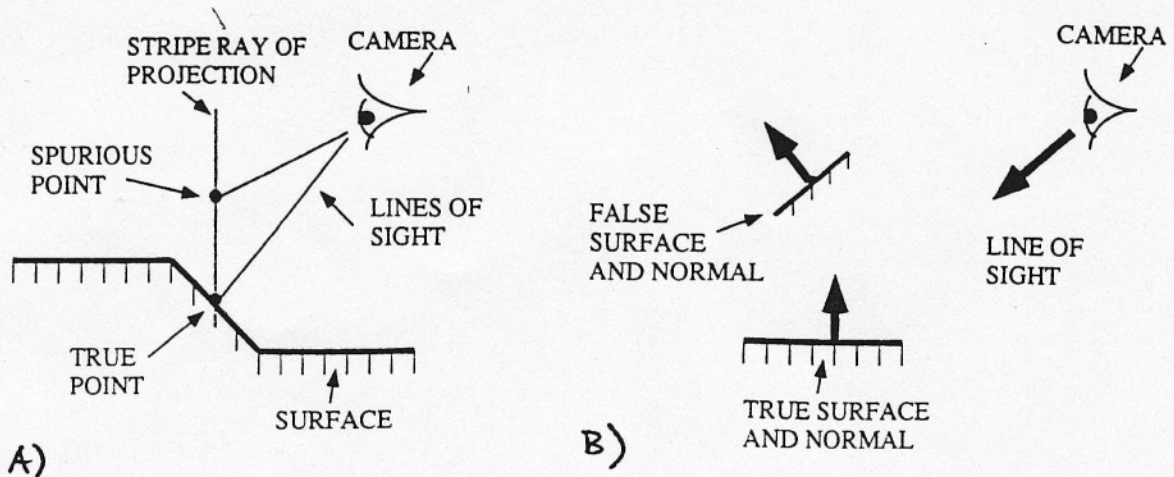


Figure 4: (a) Illumination Direction Constraint Geometry and (b) Observable Surface Constraint Geometry

the surface twice. Mathematically, each such "beam" of light projects onto a curve (usually a line) in the the sensor's projection plane. Therefore, the light stripe should intersect this curve in at most one point. When more than one point is observed, all points should be eliminated, as it is not possible to easily tell which is the correct point (brightness is no guarantee on specular surfaces). Figure 4 part (a) illustrates this constraint.

- **Observable Surface Constraint**

Adjacent stripe positions often lead to nearby spurious points forming spurious range surfaces (Figure 2 part (a) shows an example). One constraint that eliminates many of these surfaces is the requirement that the visible portion of that surface must face the observing sensor (otherwise the surface could not have been seen). Figure 4 part (b) illustrates this constraint. Hence, any local surface point whose normal  $\vec{n}_\alpha(t)$  satisfies:

$$\vec{n}_\alpha(t) \circ (\vec{P}_\alpha(t) - \vec{O}_\alpha) > 0$$

should be rejected. This constraint does not depend on having multiple cameras. Figure 4 part (b) illustrates this constraint.

- **Consistent Surface Constraint**

If a true point is observed by both cameras, then the range values ( $Z_L(t)$  and  $Z_R(t)$ ) from both cameras should be the same. If the following condition occurs:

$$|Z_L(t) - Z_R(t)| > \tau_d$$

then reject this point as being corrupted by spurious reflections.  $\tau_d$  is chosen based on the noise statistics of true range images.



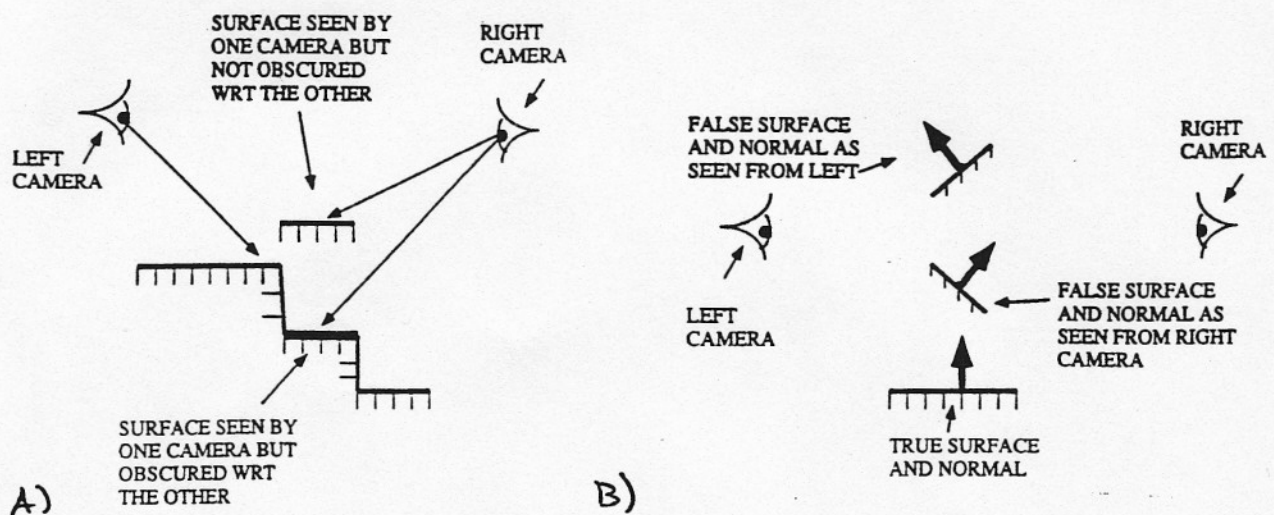


Figure 5: (a) Consistent Surface Constraint Geometry and (b) Unobscured Once Viewed Constraint Geometry

In addition to having the same  $Z$  position, the surface normals of the surfaces observed from the left and right sensors should be the same. Let  $\vec{n}_L(t)$  and  $\vec{n}_R(t)$  be the local surface normals for the left and right camera data. Then, if the following condition occurs:

$$\vec{n}_L(t) \circ \vec{n}_R(t) < \tau_n$$

then reject this point as being corrupted by spurious reflections.  $\tau_n$  is chosen based on the noise statistics of true range images; however, it may need to be set carefully, since surface normals are related to the first-order derivatives of the data and thus are more affected by noise. Figure 5 part (a) illustrates this constraint.

- **Unobscured Once Viewed Constraint**

Points that satisfy the above constraints may still be invalid, as spurious points observed by only one camera will not be eliminated by the previous constraint. However, an additional constraint can be derived from having two cameras: if the point was visible by only one camera, then there must be a valid point seen by the other camera that obscures this point. Hence, any points that are visible to one camera and are not obscured relative to the other camera, yet were not observed, are likely to be spurious points and are removed. Figure 5 part (b) illustrates this constraint.

## 4 Test Results

Figure 1 part (b) shows the range surface calculated by applying the tests to the range images from the left and right cameras shown in Figure 2 parts (a) and (b). In both of the single camera images, there are significant amounts of incorrect range data in the hole

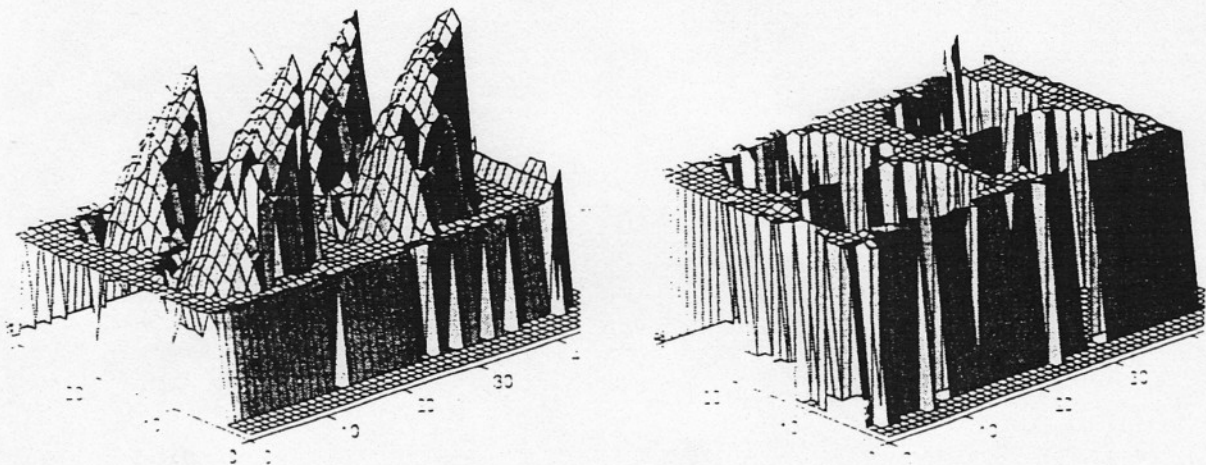


Figure 6: (a) A false range surface for a part with many holes when observed from the right camera and (b) a range surface resulting from the processing described in this paper.

Figure 6 part (b) shows the range image of a part with holes of different depths and Figure 6 part (a) shows the right range image without the rejection technique. There is a dramatic rejection of the spurious range values, although, with the rejection technique, some of the true range points have also been eliminated here. This has caused a "ragged" appearance to the object surface, but the remaining range points have the correct height.

## 5 Conclusion

As shown in the previous section, the tests eliminate many of the specular reflections arising on range scanning of metallic parts. If some information about the parts being scanned were known, then it might be possible to design further object-specific tests to reject other spurious range values.

If the noise statistics of the range images are high, then it is possible for some false range values to be accepted even if a stripe is observed by both cameras. This is because the thresholds  $\tau_d$  and  $\tau_n$  must be set so that true surface points are not rejected. Then, it becomes more likely that false range values will pass the tests. However, as seen in the tests shown in the previous section, the number of spurious range points passing both tests was minimal.

The techniques for eliminating spurious range values were described for two cameras, but it is possible to use more than two cameras. There are several real advantages to using additional cameras (at the cost of extra equipment and processing):

- Specular reflections are not always likely to be detected, so extra cameras makes it more likely to be able to apply these techniques.

- If two specular reflections are detected that lead to the same false range value, a third identical false range value is unlikely.
- Light stripe ranging requires that the surface measured to be both accessible by the illumination and visible by the camera. Additional cameras ensure that the true stripe is more likely to be seen.
- In addition to the rejection of spurious range values, having additional true measurements means that measurement error can be reduced by combining the separate measurements.

However, having additional cameras also makes it more likely that a spurious reflection will occur and be observed, which might cause true data to also be rejected.

While the rejection algorithms were described here as if complete range images were obtained before the rejection algorithms are checked, it is possible to apply all but the Once Viewed Constraint on a stripe-by-stripe basis, requiring only buffering sufficient stripes that the surface normals can be estimated locally. These methods can integrate easily with standard data buffering methods and thus still allow video-rate range calculation.

## Acknowledgements

The work for this project was funded by a grant by the European Institute of Technology, a SERC/ACME grant GR/H 86905 and the University of Edinburgh.

## References

- [1] Besl, P. J. *Range Imaging Sensors*, General Motors Research Publication GMR-6090, General Motors Research Laboratories, Warren, Michigan, 1988.
- [2] Fisher, R. B., Naidu, D. K., Singhal, D., *Rejection Of Spurious Reflections In Structured Illumination Range Finders*, patent pending, 1993.
- [3] Rioux, M., and Blais, F. *Compact three-dimensional camera for robotic applications*. J. Opt. Soc. Am. A3(9): 1518-1521, 1986.
- [4] White, S. J. *High Speed Scanning Method and Apparatus*. U.S. Patent No. 4,498,778, Technical Arts Corp., 1985.
- [5] White, S. J. *Method and Apparatus for Locating Center of Reference Pulse in a Measurement System*. U.S. Patent No. 4,628,469, Technical Arts Corp., 1986.